Measurement of Three-Dimensional Rotational and Translational Displacements using a Multi-Facet Mirror

Won Shik Park and Hyungsuck Cho

Dept. of Mechanical Engineering, Korea Advanced Institute of Science and Technology
373-1, Kusong-dong, Yusong-gu, Taejeon 305-701, Korea

ABSTRACT

A measurement system that can measure the six-degree-of-freedom motions of arbitrary objects is proposed. The measurement system utilizes a special mirror looking like a triangular pyramid and having three reflective lateral surfaces, which is to be mounted on the objects of interest. Once a laser beam illuminates the top of the mirror, the mirror reflects and splits the beam into three beams. These reflected beams are detected by three position-sensitive detectors (PSD), respectively. Based on the signal outputs of the PSDs, the three-dimensional position and orientation of the mirror can be computed, which, in turn, determines the three dimensional position and orientation of the object. This paper proposes two options in applying the measurement principle, one of which has its laser beam source fixed in space, and the other controls the translational motion of the laser beam source to track the mirror. In this paper, the principle of the measurement is proved to be valid through theoretical analysis and experiments. And the advantages and disadvantages of both options are discussed.

Keywords: 3-dimensional object pose, 6-DOF motion, 3-facet mirror, position-sensitive detector (PSD)

1 INTRODUCTION

Optical instruments such as laser interferometers [1,2], laser doppler vibrometers [3], etc. for measuring micro or nano scale motions are widely used in a variety of industrial areas. These instruments, which are basically for 1-D measurement, show very high precision, even the order of nanometers in translation. For higher dimensional measurement such as 2- or 3-D position plus rotation, it is necessary to integrate several laser interferometers and laser doppler vibrometers, which is a very difficult task since it becomes significantly more difficult to measure the motions of any object with increases of even one-DOF. Though there have been great deals of demands for the measurement methods to obtain multi-degree-of-freedom, only a few methods have been developed for some limited applications. Lee et al. [4] investigated the possibility of their new optical system consisting of a laser source, four quad-detectors,

Prof. Hyungsuck Cho(correspondence), E-mail: hscho@lca.kaist.ac.kr, WWW: http://lca.kaist.ac.kr, Tel: +82-42-869-3213, Fax: +82-42-869-3210

Optomechatronic Systems IV, George K. Knopf, Editor, Proceedings of SPIE
Vol. 5264 (2003) © 2003 SPIE · 0277-786X/03/$15.00

four beam splitters, etc. to measure 6-DOF simultaneously. Their method mounts four beam splitters on the object of interest to form a light path emitted from a laser source to four quad-detectors. Based on the precision of their quad-detectors, they estimated the translational and rotational resolutions to be 0.05 μm and 0.25 μrad, respectively. But the mounting of four beam splitters leads to large additive weight of the object, thus the dynamic characteristics of the object may be largely affected.

In this paper, a new measurement method is proposed that can simultaneously measure the 3-D position and orientation of rigid bodies with the precision order of micrometers and microradians. The sensor system utilizes a laser source, a specially fabricated mirror, and three PSDs. The specially fabricated mirror, called three-facet mirror in this paper, looks like a triangular pyramid having an equilateral cross-section. We mount this mirror on the objects of interest, illuminate the mirror with a He-Ne laser beam, and then detect the beams reflected from the mirror with PSDs. From the output signals of the PSDs, we can calculate the 3-D position and orientation of the three-facet mirror, thus enabling us to obtain the 3-D position and orientation of the objects. This method utilizes a small and light mirror, thus the mirror affects the dynamic characteristics of the object much less than that of Lee et al.'s method [4].

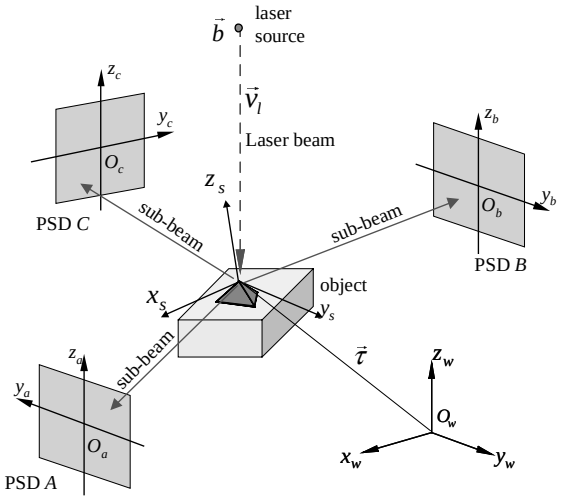

Figure 1 Schematic drawing of the sensing system

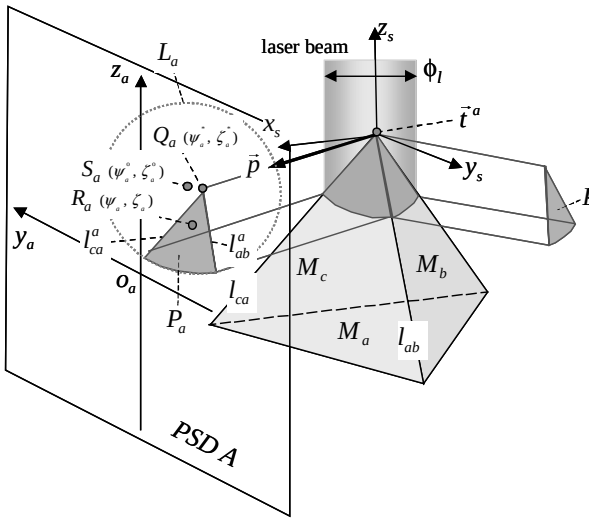

Figure 2 3-facet mirror and PSD A

2 PRINCIPLE OF SENSOR SYSTEM

2.1 System configuration

The schematic configuration of the proposed sensor system is shown in Figure 1. In the figure, the sensor system is composed of a mirror of pyramidal shape, a laser source, and three position-sensitive detectors (PSDs). The mirror has an equilateral triangular cross-section, which is referred to as three-facet mirror since it has three reflective lateral surfaces. Its reflective surfaces are inclined 45° to its bottom surface, respectively, and the three bottom edges make

equal angle of 60° to each other. As shown in Figure 2, once a laser beam illuminates the top of the three-facet mirror, the reflective surfaces M_a, M_b, and M_c split the laser beam into three beams, which are called subbeams in this paper. And the subbeams impinge the sensitive areas of the PSDs, from which the PSDs detect the positions of the spots of the subbeams as well as the incident light powers. If the three-facet mirror moves in any way, the positions of the beam spots on PSDs and their incident light powers vary in some corresponding way. If there exists some proper relationship between the displacements of the mirror and the PSDs' outputs, we may utilize this optical principle to estimate the three-dimensional displacements of the mirror from the PSDs' outputs. In the following sections, we construct a mathematical model of the relationship and based upon this, theoretically check if the proposed principle is valid.

Figure 3 shows the planar view of the sensor system with its laser source omitted for presentation. Here, the laser beam is kept vertical to the reference plane of the sensor system, which is defined by three origins of the PSDs. As shown in the figure, three PSDs are located at the same distance R_{PSD} from the origin of the sensor system o_w, around which the origins of the PSDs make an equal angle 120° with each other. In the previous study [5], it has been presented that the angles between the PSDs θ_{ab} and θ_{ac} are not so important, but the distance from the center to the PSDs R_{PSD} affects the angular resolution of the sensor. In this paper, the issues about the system parameters and their effects are not presented, but we focus on the principle and its variations that properly adapt to given problems.

2.2 Sensor model

The PSDs are illuminated by the subbeams and provide the output signals about the 2-D positions and incident light powers of the beam spots. Within the beam spots, irradiance distributions look like pie-pieces as shown in Figure 2. If the three-facet mirror translates or rotates, the irradiance distributions on the PSDs vary in general so that the PSDs provide the changes in the 2-D coordinates and incident light power of the beam spots. In this section, the mathematical relationship between the 3-D pose of three-facet mirror and the PSD outputs is derived, which is a function that calculates the PSD outputs from given 3-D position and orientation of three-facet mirror. The derivation is based on light path tracing from the source to the destination, in which a laser beam is regarded as a set of straight lines. For simplicity of the model, diffractive effect is neglected and on account of space consideration, the derivation for one detector, PSD A, is presented in this paper.

The system model $\mathbf{J}_f$ relating the three-dimensional pose of three-facet mirror to the outputs of three PSDs can be expressed as

$$\vec{\xi} = \mathbf{J}_f(\vec{\tau}) \tag{1}$$

where $\vec{\xi}$ and $\vec{\tau}$ represent the output and input of the sensor, respectively, defined as follows.

$$\vec{\xi} = [\psi_a \;\; \zeta_a \;\; \Phi_a^* \;\; \psi_b \;\; \zeta_b \;\; \Phi_b^* \;\; \psi_c \;\; \zeta_c \;\; \Phi_c^*]^T \tag{2}$$

$$\vec{\tau} = [t_x \quad t_y \quad t_z \quad \gamma \quad \beta \quad \alpha \quad b_x \quad b_y]^T . \tag{3}$$

Here the components of $\vec{\xi}$ are the output signals provided by the PSDs. (ψ_a, ζ_a) represents the 2-D coordinate of the beam spot impinging on *PSD A* with respect to the coordinate system o_a defined on *PSD A* and Φ_a^* represents the incident light power on the same detector. Similarly, (ψ_b, ζ_b), Φ_b^*, (ψ_c, ζ_c), and Φ_c^* represent the outputs of *PSD B* and *C* with respect to their corresponding coordinate systems o_b and o_c. $\vec{\tau}$ consists of the 6-DOF components of three-facet mirror. t_x, t_y, and t_z are the coordinates of the top of the mirror with respect to the reference frame o_w and γ, β, and α are the roll, pitch, and yaw angles, respectively. The definition of these six components corresponds to the relative linear and angular displacement between the object frame o_s defined at the vertex of the mirror and the reference frame o_w. It is noted that the sensor input $\vec{\tau}$ includes (b_x, b_y), which is the 2-D coordinate of the laser beam center defined as the intersection between the laser beam center and $x_w y_w$-plane. This is represented with respect to the reference frame o_w. The reason why $\vec{\tau}$ includes (b_x, b_y) is based on theoretical analysis to be explained in the following section and to present that $\mathbf{J}_f$ provides a one-to-one mapping between $\vec{\xi}$ and $\vec{\tau}$.

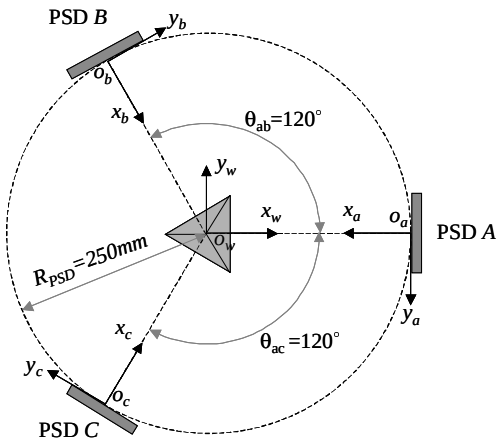

Figure 3 Planar view of the sensor system

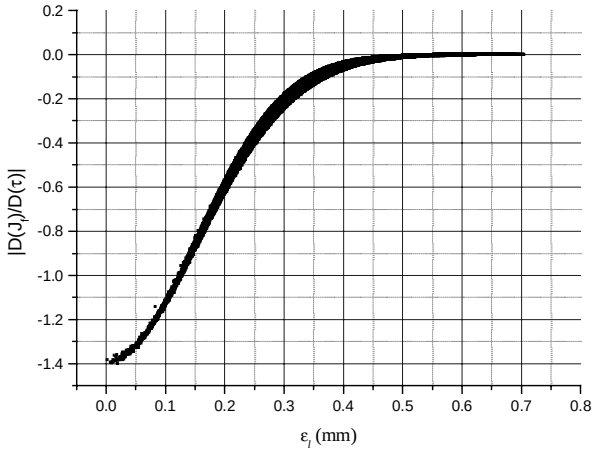

Figure 4 Jacobians of $\mathbf{J}_f$

$\mathbf{J}_f$ has eight input variables and nine output variables. For a one-to-one mapping between input variables and output variables, it is necessary that there should be a constraint that reduces the number of independent output variables. It is obvious that the sum of the incident light powers on the PSDs is constant or rather the same as the power output of the laser source if the attenuation at the mirror surface is negligible. Thus,

$$\Phi_a^* + \Phi_b^* + \Phi_c^* = P , \tag{4}$$

by which the number of independent output variables reduces to eight.

To derive the model that predicts the PSDs' output, $\vec{\xi}$, from the mirror pose plus the laser beam position, $\vec{\tau}$, we

should (1) identify the shape of the beam spot, (2) obtain the irradiance distribution, and (3) calculate the mass and center of mass of the irradiance distribution within the spot for each PSD. These procedures are to be described in the followings.

Shapes of beam spots on the detectors

Figure 2 shows a situation, in which a subbeam reflected from M_a impinges on *PSD A* to form a spot resembling a piece of pie, P_a. In the figure, the dotted ellipse L_a is the imaginary cross-section of the laser beam as if the laser beam were not split by the three-facet mirror but normally reflected by a planar mirror whose pose is the same as that of M_a. S_a is the center of the dotted ellipse L_a and also the projected image of the center of the laser beam. Two edges of P_a, l_{ab}^a and l_{ca}^a, are the projected images of the edges of the 3-facet mirror, l_{ab} and l_{ca}. L_a including the arc of P_a is defined as the projected image of the boundary of the laser beam defined by beam diameter ϕ_l. Q_a, the intersection of l_{ab}^a and l_{ca}^a, is the point projected from the top of the mirror, as shown in the figure. If the center of laser beam coincides with the mirror top, then Q_a and S_a are located at the same position. R_a is the light centroid of P_a, which is the reading of the 2-D position of the beam spot on *PSD A*. More details on the prediction of the P_a including R_a, Q_a and S_a are referred to the previous literature [5, 6].

Intensity distributions on the detectors

First, we model the original laser beam of Gaussian intensity distribution from a source whose direction vector is $\vec{v}_l$ and the position of source point is $\vec{b}$. As described above, the direction of the laser beam is kept vertical. Thus, $\vec{v}_l^w$ can be expressed as

$$\vec{v}_l^w = [0 \quad 0 \quad -1]^T \tag{5}$$

The intensity distribution within the beam is distributed in Gaussian functional form given by

$$I(r) = \frac{8P}{\pi\phi_l^2} \exp\left(-\frac{8r^2}{\phi_l^2} \right). \tag{6}$$

Here, P represents the power of the laser beam, ϕ_l the diameter of the laser beam, and r the radial distance from the center axis of the laser beam to any point of interest.

As shown in Figure 2, the circular cross-sectional profile of the Gaussian beam is somewhat changed into an elliptical one, which depends on the angle of incidence of the subbeam. The irradiance distribution within the elliptical beam profile of P_a can be expressed as follows:

$$I_a(r_a) = \frac{\vec{p} \cdot \hat{x}_a}{\|\vec{p}\|} I(r_a) \tag{7}$$

where $\hat{x}_a$ is the unit surface normal vector of PSD A and $\vec{p} = [p_x \quad p_y \quad p_z]^T$ is the direction vector of the subbeam

A with respect to o_a, which can be obtained by applying the reflection law [7] to the direction vector of the original laser beam. And it should be noted that r_a is not the radial distance as used in Eq. (6), but somewhat different term, called modified radial distances in this paper and defined as follows:

$$r_a = \sqrt{(y_a - \psi_a^o)^2 \frac{p_x^2}{p_x^2 + p_y^2} + (z_a - \zeta_a^o)^2 \frac{p_x^2}{p_x^2 + p_z^2}} \tag{8}$$

Mass and center of mass of the irradiance distribution

As described above, the locations (ψ_a, ζ_a), (ψ_b, ζ_b), and (ψ_c, ζ_c) are the centers of mass of the irradiance distribution within P_a, P_b, and P_c. For PSD A, (ψ_a, ζ_a) can be computed as follows:

$$\psi_a = \frac{\iint_{P_a} y_a I_a(r_a) dy_a dz_a}{\iint_{P_a} I_a(r_a) dy_a dz_a}, \qquad \zeta_a = \frac{\iint_{P_a} z_a I_a(r_a) dy_a dz_a}{\iint_{P_a} I_a(r_a) dy_a dz_a} \tag{9}$$

At this stage, we have completed modeling the relationship between the 3-dimensional pose, t_x, t_y, t_z, γ, β, and α, and the PSD outputs, $(\psi_a, \zeta_a, \Phi_a^*)$, $(\psi_b, \zeta_b, \Phi_b^*)$, and $(\psi_c, \zeta_c, \Phi_c^*)$. The 2-dimensional position of the laser beam (b_x, b_y) takes part with in the input side of the model, while it is not so important as others. When actual measurement is performed with the proposed sensor system, it is necessary to perform an inversion of the above model, i.e., calculation of t_x, t_y, t_z, γ, β, and α with given $(\psi_a, \zeta_a, \Phi_a^*)$, $(\psi_b, \zeta_b, \Phi_b^*)$, and $(\psi_c, \zeta_c, \Phi_c^*)$. The inversion is performed through a numerical way, the Newton's method [8], through which we have successfully obtained the solution, t_x, t_y, t_z, γ, β, and α, from given $(\psi_a, \zeta_a, \Phi_a^*)$, $(\psi_b, \zeta_b, \Phi_b^*)$, and $(\psi_c, \zeta_c, \Phi_c^*)$ in the experiments to be explained in section 3.

2.3 Existence of the inverse function of the sensor model

In this section, the existence and uniqueness of the inverse function of $\mathbf{J}_f$ is examined. For the examination, inverse function theorem [9] is applied. For the purpose, it should be shown that there exists a set of functions $\{f_1, \cdots, f_8\}$ that is a subset of the PSD outputs $\{\psi_a, \zeta_a, \Phi_a^*, \psi_b, \zeta_b, \Phi_b^*, \psi_c, \zeta_c, \Phi_c^*\}$ satisfying

$$\left.\frac{\partial(f_1, \cdots, f_8)}{\partial(t_x, \cdots, b_y)}\right|_{\vec{\tau}} = \begin{vmatrix} \frac{\partial f_1}{\partial t_x}(\vec{\tau}) & \cdots & \frac{\partial f_1}{\partial b_y}(\vec{\tau}) \\ \vdots & \ddots & \vdots \\ \frac{\partial f_1}{\partial t_x}(\vec{\tau}) & \cdots & \frac{\partial f_1}{\partial b_y}(\vec{\tau}) \end{vmatrix} \neq 0 \tag{10}$$

for every $\vec{\tau}$ in measurement range. From (4), it is expected that one of Φ_a^*, Φ_b^*, and Φ_c^* is redundant for unique $\vec{\tau}$ if the power of laser beam P is constant, which is a reasonable condition if we use some properly stabilized laser source. Here, Φ_c^* is omitted and then to check the condition in Eq. (10) as follows:

$$\left.\frac{\partial(\psi_a,\cdots,\zeta_c)}{\partial(t_x,\cdots,b_y)}\right|_{\vec{\tau}} = \begin{vmatrix} \frac{\partial \psi_a}{\partial t_x}(\vec{\tau}) & \cdots & \frac{\partial \psi_a}{\partial b_y}(\vec{\tau}) \\ \vdots & \ddots & \vdots \\ \frac{\partial \zeta_c}{\partial t_x}(\vec{\tau}) & \cdots & \frac{\partial \zeta_c}{\partial b_y}(\vec{\tau}) \end{vmatrix}. \tag{11}$$

Figure 4 shows the determinant values in Eq. (11) with respect to the relative distance between the laser beam center and the vertex of three-facet mirror ε_l defined as

$$\varepsilon_l = \{(t_x - b_x)^2 + (t_y - b_y)^2\}^{1/2}. \tag{12}$$

In the evaluation, the system parameters are given as in Figure 3 and Table 1 except laser power *P* and beam diameter ϕ_l. Here the laser power *P* is assumed to be 1mW and the beam diameter ϕ_l is to be 1mm. And $\vec{\tau}$, the 6-DOF pose of three-facet mirror and 2-dimensional position of the laser beam, has been chosen randomly within the measurement range condition. As shown in Figure 4, the jacobian is negative definite over the range, thus the sensor model $\mathbf{J}_f$ is proved to have unique inverse function within the measurement range. The number of points randomly examined is over 200000, whose neighborhoods are expected to sufficiently cover the input space.

Table 1 Specifications of the experimental system

Components	Specifications		
He-Ne Laser	Power		0.3 mW
	Beam diameter		0.85 mm
	Beam orientation at 3-facet mirror		Vertical (const.)
3-facet mirror	Azimuth of surface normal		45°
	Longitudinal distance between surface normals		120°
	Surface flatness		λ/10 at 632.8 nm
PSD	Size of sensitive area		13 mm x 13 mm
	Layout	Radial distance from the system origin	250 mm
		Longitudinal distance between PSDs	120°
		Orientations	See Figure 3

3 EXPERIMENTS

In order to verify the principle and effectiveness of the proposed measurement method, we have implemented an experimental system and performed a series of experiments. The configuration of the experimental system is shown as in Figure 3 and Table 1. Figure 5 shows the actual appearance of the experimental system and a closer look of three-facet mirror. As shown in section 2.3, the proposed method can estimate the 6-DOF of three-facet mirror from the PSD outputs, regardless of the 2-D position of the laser beam, if the beam illuminates the top of the mirror. In this section,

we present two kinds of variation of the proposed method, one of which uses a laser beam of fixed position and the other controls the laser beam to track the top of the mirror. The former is advantageous for fast objects and the latter is for a larger measurement range.

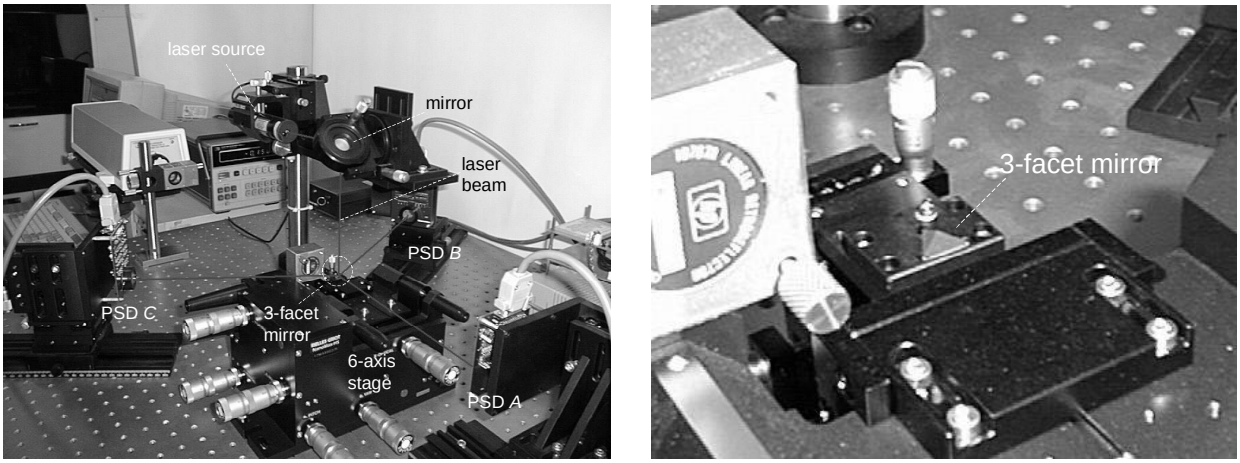

Figure 5 Photography of the experimental system

3.1 6-DOF pose estimation with a fixed laser beam

If we need to measure some motion of small range that can be covered by the cross-sectional area of the laser beam, the laser beam would be better to be fixed at a position while its orientation is also fixed as vertical. It is quite natural to locate the laser beam at the center of the sensor system so that $(b_x,\ b_y) = (0,\ 0)$. Figure 6 shows some measurement ranges of the sensor system when its laser beam is fixed at the center, in which each plot presents measurement range of some 2-DOF motion while the rest 4-DOF components are set to zero. In the plot showing the range of $x_w y_w$ planar motion, we can see the measurement range is much smaller than the laser beam profile. This is because as the top of the mirror moves outward the beam, some of the three PSDs will get so weak incident light that its signal-to-noise ratio gets too low. Thus, the measurement range in $x_w y_w$-direction is limited by the S/N ratio of the PSDs. On the other hand, the other motions such as z_w-translation and rotations are limited by the size of sensitive area of PSD.

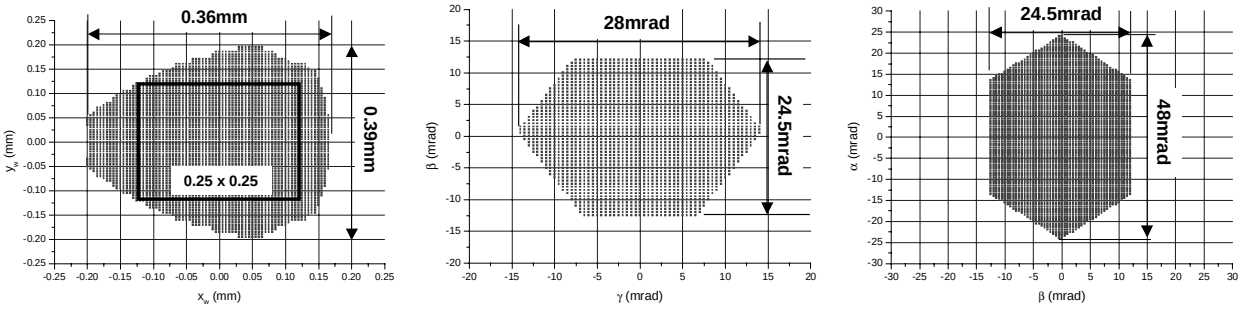

Figure 6 Measurement range with a fixed laser beam

Figure 7 - Figure 9 present some of our experimental results for single axis motions and multi-axis motions, while the errors in 6-DOF are also presented. From the error plots, we can see that the proposed method successfully obtains the translational and rotational displacements from the PSD signals with limited cross-axial errors.

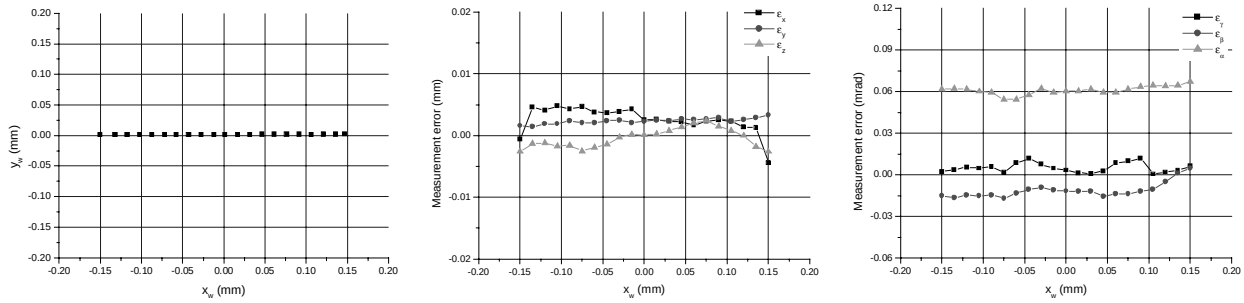

Figure 7 Translation in x_w-axis

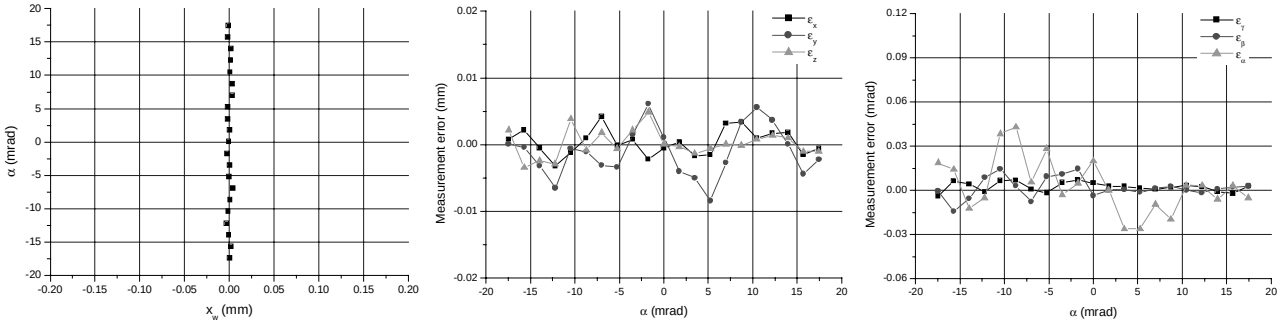

Figure 8 Rotation around z_w-axis

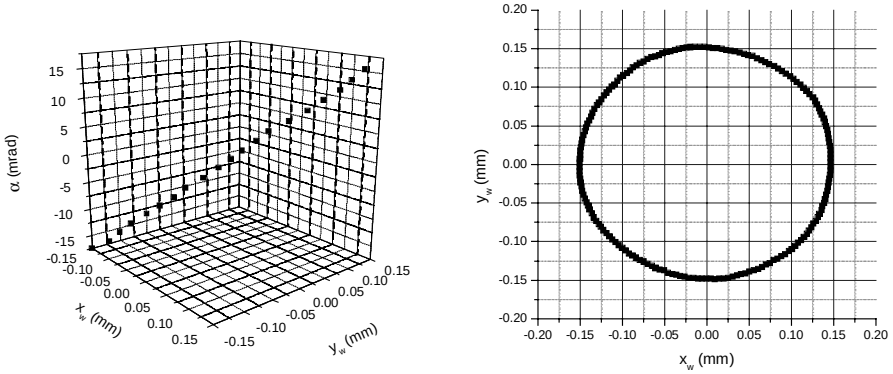

Figure 9 Multi-DOF motions

3.2 6-DOF pose estimation with beam position adjustment

The proposed method can be easily modified to achieve a larger measurement range in $x_w y_w$-direction. The laser beam source is mounted on a two-axis translation stage so that the beam can track the top of three-facet mirror. In this method, we adopt a feedback loop to adjust the 2-D position of the laser beam to three-facet mirror. The error signals indicating the offset between the center of the laser beam and the top of three-facet mirror are obtained by comparing the incident light power shares among the PSDs. This is based on that

$$(b_x, b_y) \approx (t_x, t_y) \quad \text{if} \quad \Phi_a^* = \Phi_b^* = \Phi_c^* \quad \text{and if} \quad \gamma, \beta, \alpha < \varepsilon \,. \tag{13}$$

For example, if all of roll, pitch, and yaw angles are smaller than 10mrad, which is 0.573 degree, then we have the tracking error, the offset between the laser beam center and the top of the mirror, less than 0.89μm. For an actual feedback signal, we define some indices as follows:

$$\chi_{x_w} = \frac{\Phi_a^* + \Phi_b^* \cdot \cos 120^\circ + \Phi_c \cdot \cos 120^\circ}{\Phi_a^* + \Phi_b^* + \Phi_c^*}, \quad \chi_{y_w} = \frac{\Phi_b^* \cdot \sin 120^\circ - \Phi_c^* \cdot \sin 120^\circ}{\Phi_a^* + \Phi_b^* + \Phi_c^*}. \tag{14}$$

If χ_{x_w} is positive, we have to adjust the laser beam in negative x_w-direction, or if χ_{x_w} is negative, the beam should go in positive x_w-direction. And for χ_{y_w}, similar way of adjustment is used. And the magnitude of χ_{x_w} and χ_{y_w} represent the distance between the laser beam center and the top of the mirror. Thus it can be used as the proportional gain for P-control algorithm.

Figure 10 shows the measurement range in $x_w y_w$-direction achieved through the mirror tracking, in which the system parameters are the same as those of the method using a fixed laser beam as shown in Figure 3 and Table 1. As shown in the figure, the measurement range in $x_w y_w$-direction has been remarkably enlarged. In this method, the measurement range is not defined by the S/N ratio of the PSDs but the size of sensitive area of the PSDs.

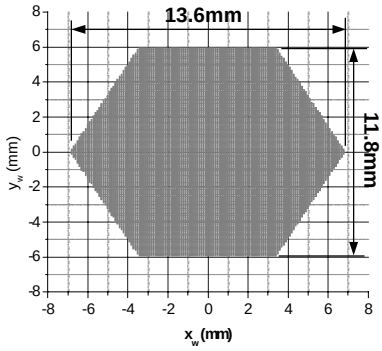

Figure 10 Measurement range in $x_w y_w$-plane motion with beam position adjustment

Figure 11 shows the experimental results for x_w and y_w-direction. As shown in the figure, the proposed method with mirror tracking has successfully measured the motions in a larger range than that with a fixed laser beam, while the

measured range is restricted within a smaller range than that shown in Figure 10 due to some limitation of experimental hardware.

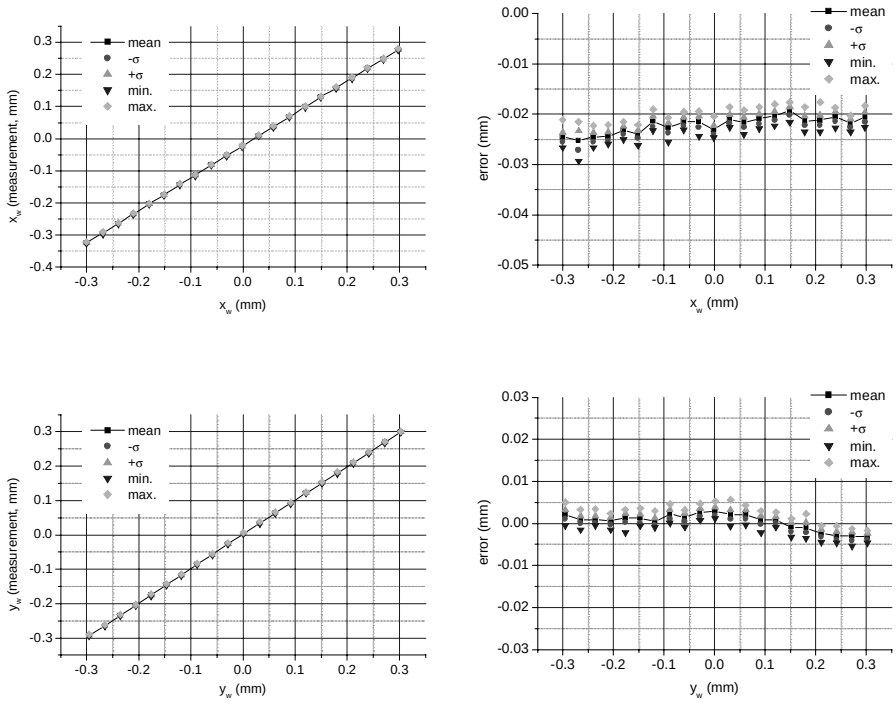

Figure 11 Experimental results for the motions in x_w and y_w-direction with mirror tracking

3.3 Sensor evaluation

In general, sensors can be evaluated by their measurement range and resolution. The sensor presented in this paper has not been optimized but an experimental setup. However, we can roughly understand its possibility and applicability to any problems that we may have to solve. Table 2 shows the measurement ranges and resolutions of the experimental system constructed in this paper. In the measurement method proposed in this paper, measurement range and resolution in 6-DOF may not be simply presented as shown in the table. The numbers listed in the table can be regarded as an outline on its performance. The measurement range in each axis has been taken as the maximum distance in the direction of interest, while other axes were set to their origin. Thus the ranges may vary when other axes are elsewhere. The resolutions in each axis also may vary with respect to the 6-DOF pose of the mirror. Thus to obtain the most representative quantity about the resolutions for six axes, we obtain a number of repeated measurement for each point in 6-DOF space, calculate the standard deviations for each point, and finally take the maximum of the standard deviations for each axis. The resolutions have been defined, in this paper, as the twice as the maximum standard deviations for each axis, which is, in other word, root-mean-squared error.

Table 2 Summary of experimental results

	x_w	y_w	z_w	γ	β	α
Range (mm, mrad)	0.36 / 13.6*	0.39 / 11.8*	12.3	28.0	24.5	48.0
Resolution (μm, μrad)	2.6	1.9	2.8	9.4	8.7	13.0

* Measurement range achieved by mirror tracking, otherwise by a fixed laser beam

4 CONCLUSIONS

The proposed principle has been proved to be valid in both theoretical and experimental ways. In theoretical analysis, we constructed a sensor model and examined it whether its Jacobian matrix is nonsingular. And in experiments, two different approaches, depending on whether the position of the laser beam tracks the mirror or not, have been examined. The one whose laser beam is not controlled has so tiny measurement range for in-plane motions that it can cover at most 0.25mm x 0.25mm square area but advantageous to fast objects of around 3kHz in bandwidth. And the other, of which the laser beam tracks the mirror, has much larger measurement range covering over 8mm x 8mm for motions in $x_w y_w$-direction but not suitable for fast objects because it needs mechanical servoing. The measurement precisions achieved in our experiments are at most 2.8μm for translation and 13.0μrad for rotation.

REFERENCES

1 L. M. Smith and C. C. Dobson, “Absolute displacement measurement using modulation of the spectrum of white light in a Michelson interferometer,” Appl. Opt., Vol. 28, pp. 3339–3342, 1989.

2 S. Hosoe, “Laser interferometric system for displacement measurement with high precision,” Nanotechnology, Vol. 2, pp. 88–95, 1991.

3 J. R. Bell and S. J. Rothberg, “Laser vibrometers and contacting transducers, target rotation and six degree-of-freedom vibration: what do we really measure?’’ J. Sound Vib., Vol. 237, No. 2, pp. 245–261, 2000.

4 N. Lee, Y. Cai, and A. Joneja, “High-resolution multidimensional displacement monitoring system,” Opt. Eng., Vol. 36, No. 8, pp. 2287–2293, 1997.

5 W. S. Park, Measurement of 6-dof motions of rigid bodies through splitting a laser beam, Ph.D. thesis, Korea Advanced Institute of Science and Technology, 2002.

6 W. S. Park and H. S. Cho, “Measurement of fine 6-degrees-of-freedom displacement of rigid bodies through splitting a laser beam: experimental investigation,” Optical Engineering, Vol. 41, No.4, pp. 860-871, April 2002.

7 M. Bass, E. W. Stryland, D. R. Williams, W. L. Wolfe, Handbook of Optics, 2nd Ed., vol. 1, McGraw-Hill, 1995.

8 W. H. Press, S. A. Teukolsky, W. T. Vetterling, and B. P. Flannery, Numerical Recipes in C, 2nd Ed., Cambridge University Press, 1992.

9 Jerrold E. Marden and Anthorny J. Tromba, Vector calculus, 2nd Ed., Freeman, 1981.